Electronic Supplementary Information (ESI)

Solubility improvement of curcumin with amino acids

Anilkumar Gunnam,[a] and Ashwini Nangia*[,a,b]

School of Chemistry, University of Hyderabad, Prof. C. R. Rao Road, Gachibowli, Central University P.O., Hyderabad 500 046, India
E-mail: ashwini.nangia@gmail.com

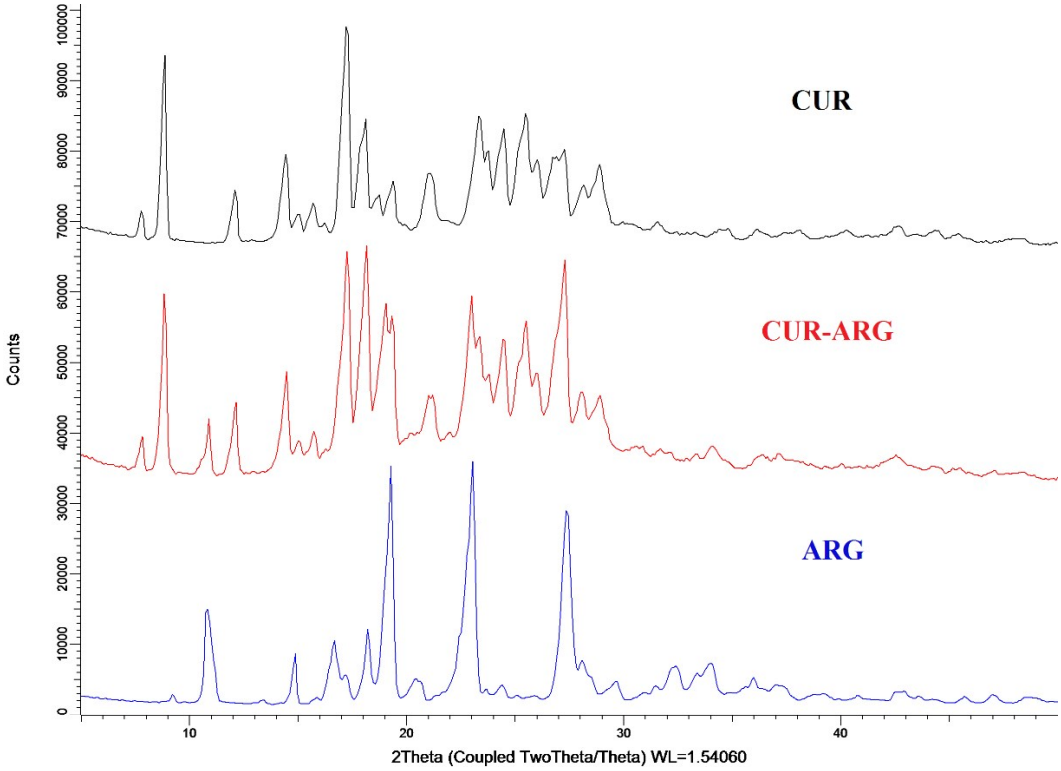

Figure S1a: PXRD overlay of CUR-ARG physical mixture with CUR and ARG

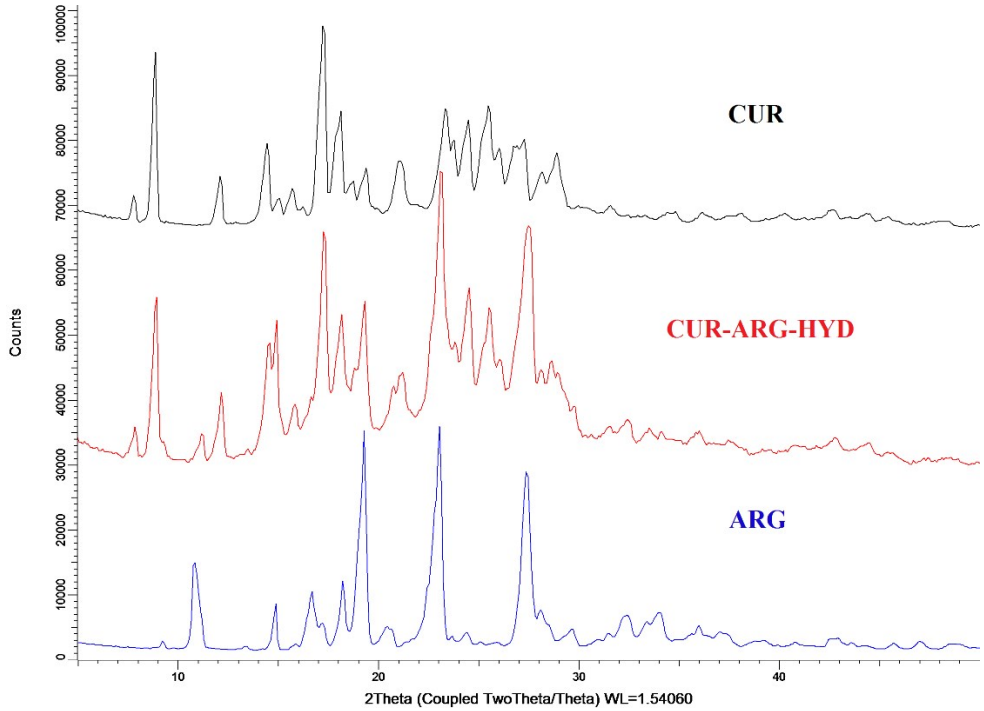

Figure S1b: PXRD overlay of CUR-ARG-HYD physical mixture with CUR and ARG

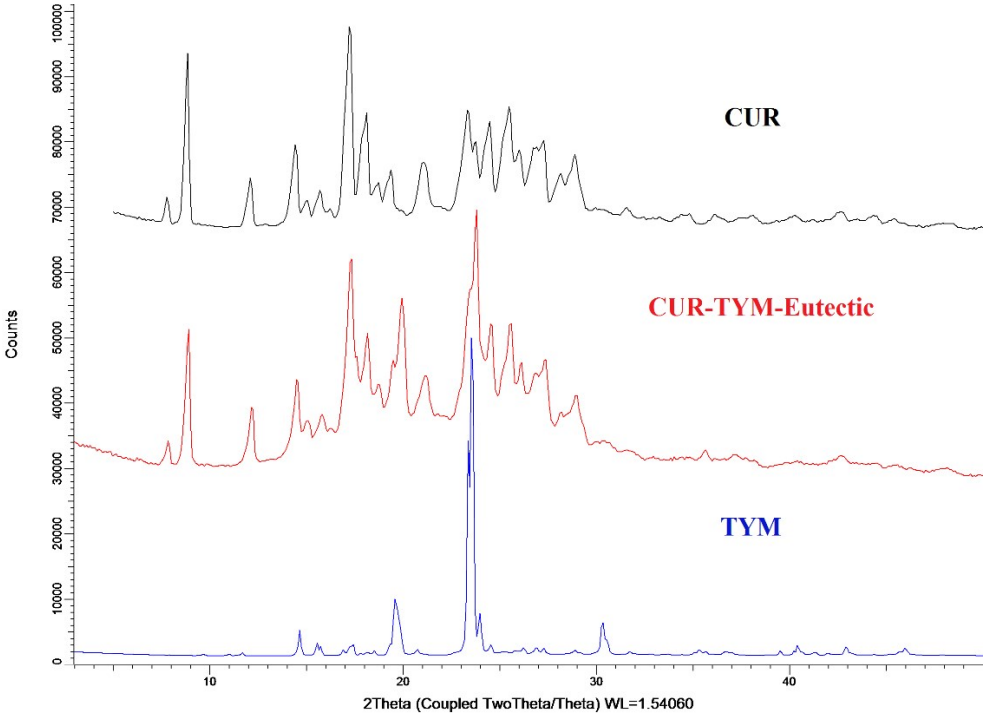

Figure S1c: PXRD overlay of CUR-TYM eutectic with CUR and TYM

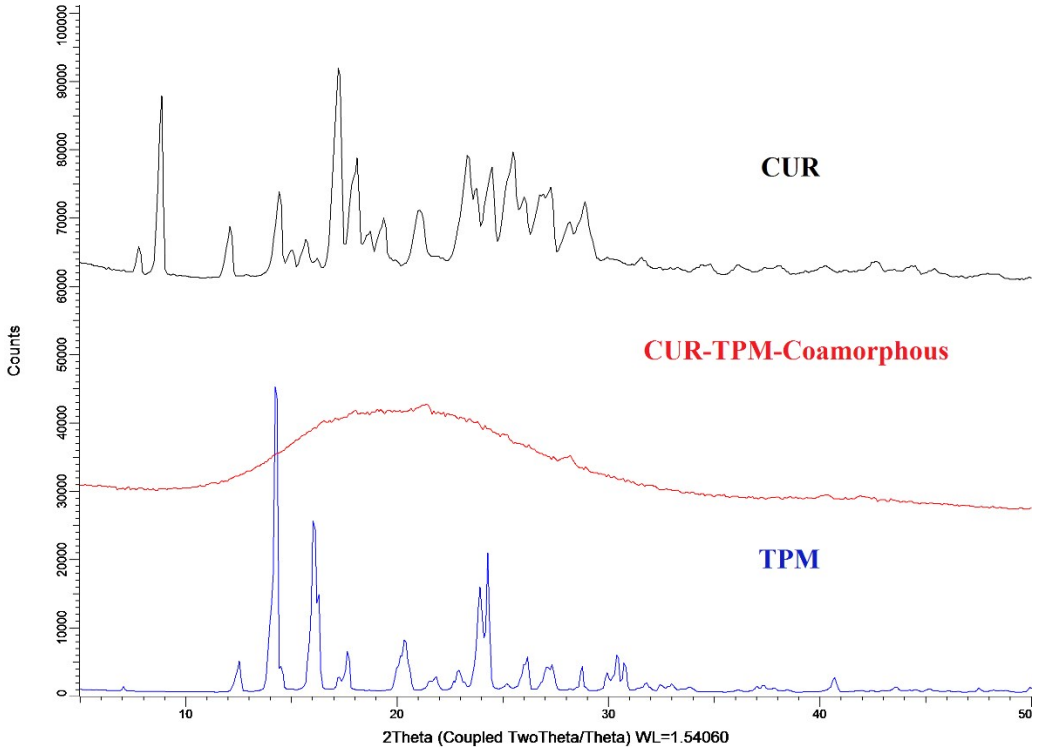

Figure S1d: PXRD overlay of CUR-TPM co-amorphous with CUR and TPM

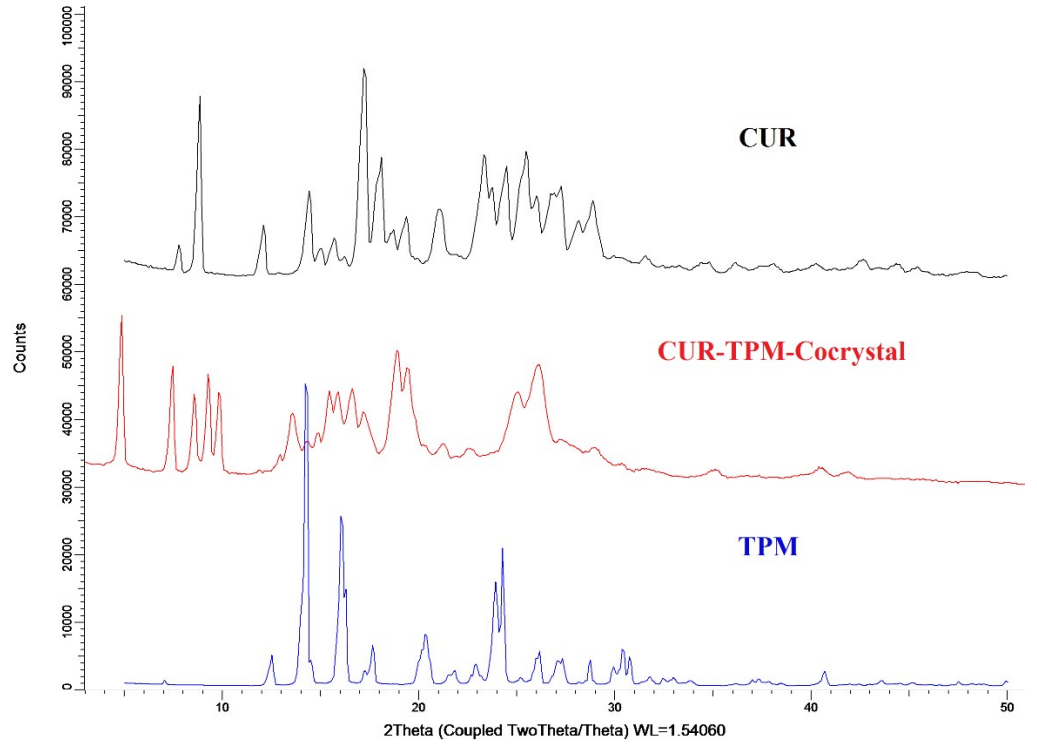

Figure S1e: PXRD overlay of CUR-TPM cocrystal with CUR and TPM

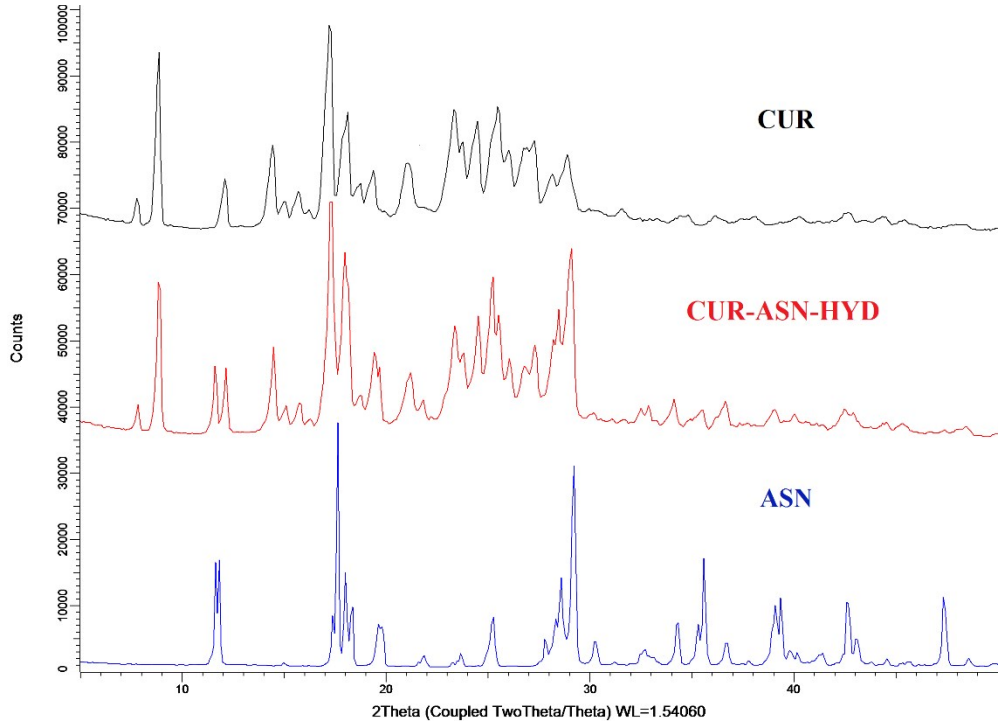

Figure S1f: PXRD overlay of CUR-ASN-HYD physical mixture with CUR and ASN

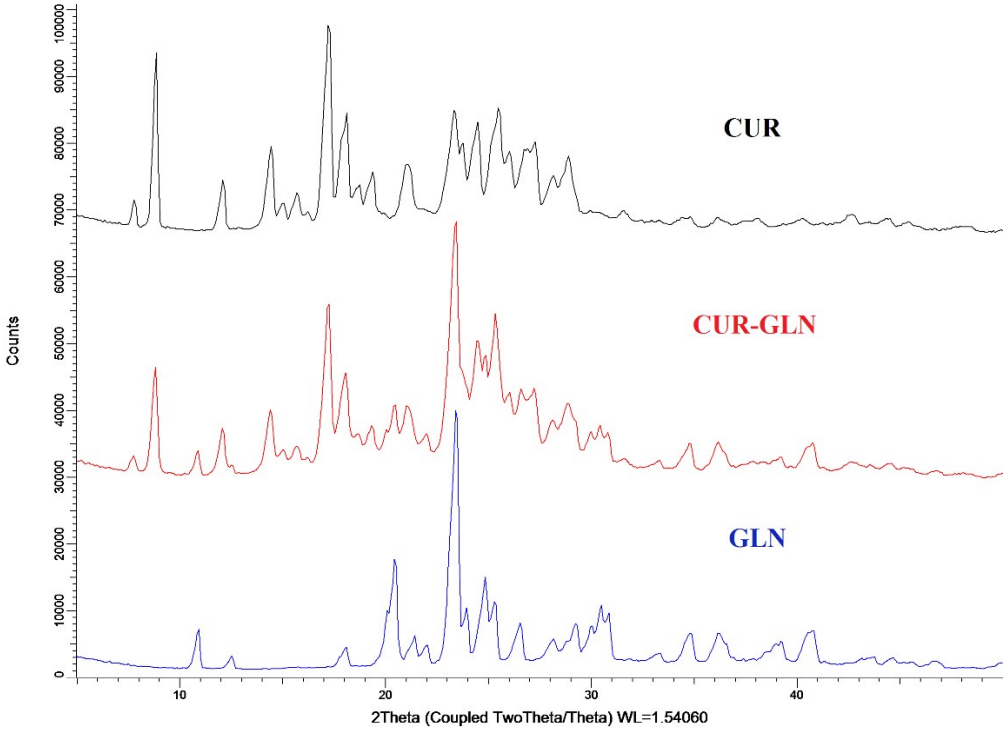

Figure S1g: PXRD overlay of CUR-GLN physical mixture with CUR and GLN

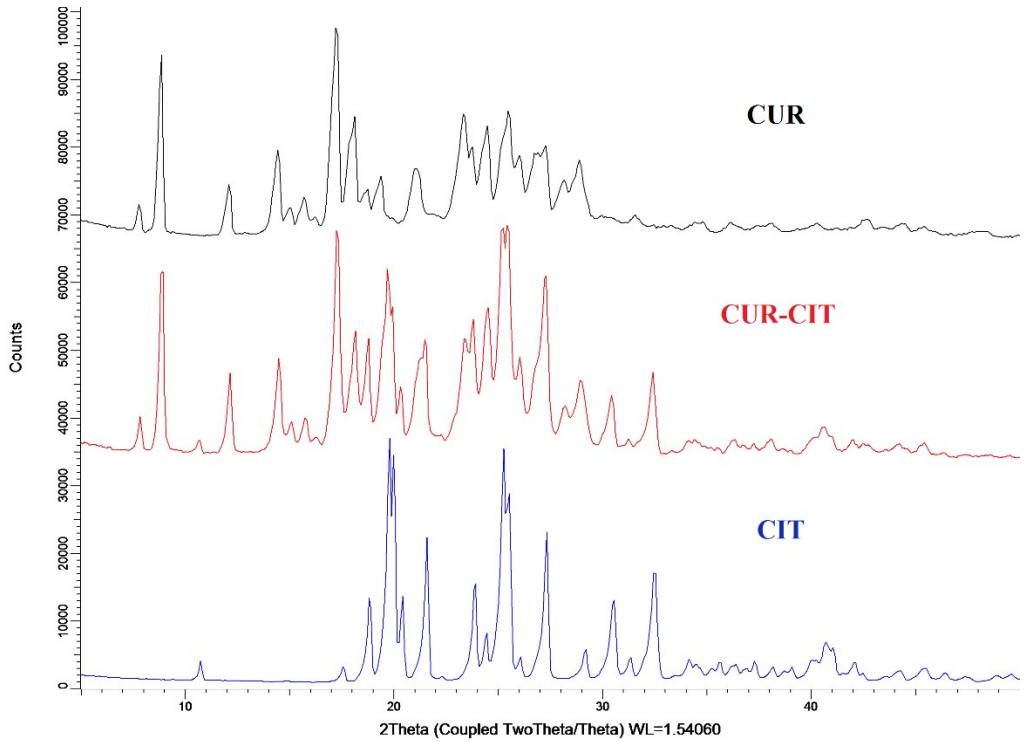

Figure S1h: PXRD overlay of CUR-CIT physical mixture with CUR and CIT

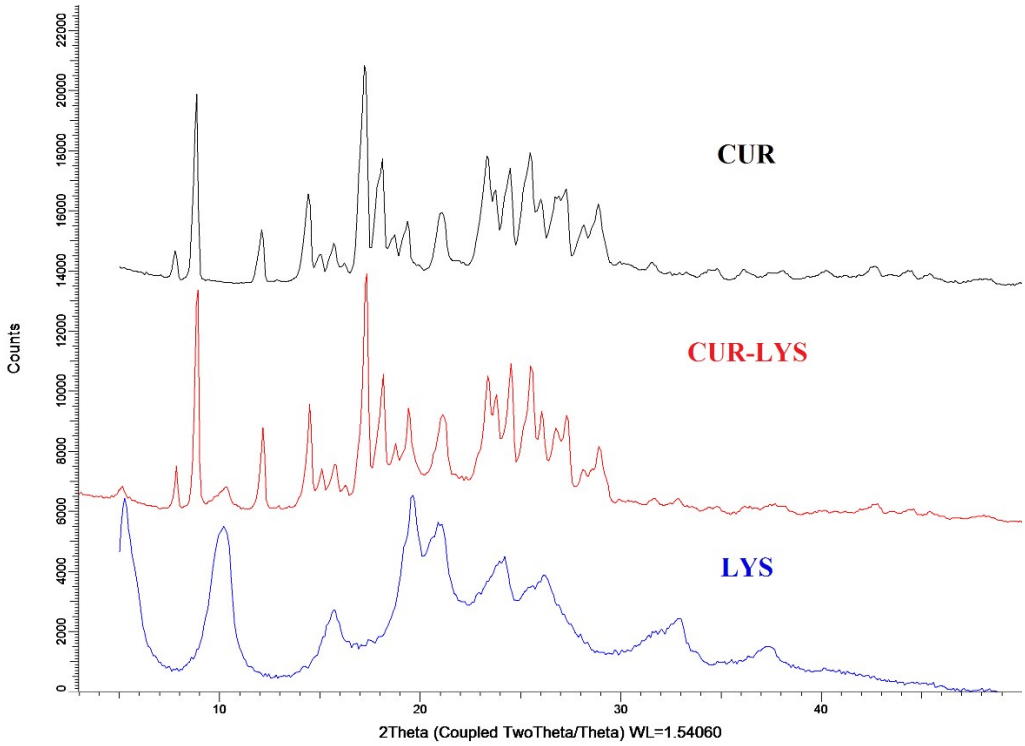

Figure S1i: PXRD overlay of CUR-LYS physical mixture with CUR and LYS

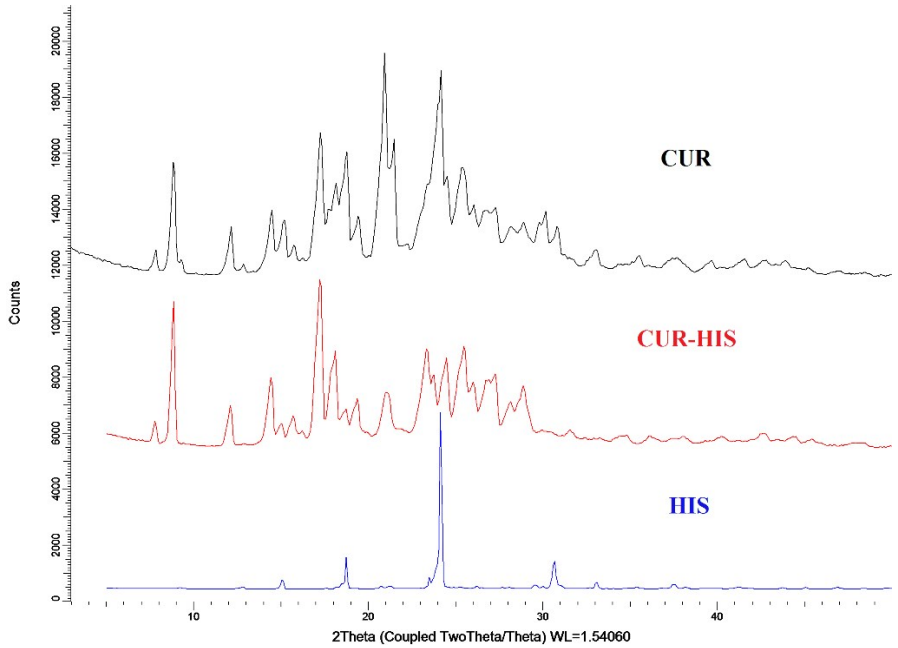

Figure S1j: PXRD overlay of CUR-HIS physical mixture with CUR and HIS

Figure S1: PXRD overlays of CUR multicomponent systems with CUR and its corresponding coformers

Table S1 Weight loss in TGA of CUR amino acid hydrates

Compound	Initial weight (in mg)	% Loss of water	Weight loss (in mg)	Equivalents of water molecules by TGA
CUR-ASN-HYD	3.87	8.9	0.34 (at 90 – 140 °C)	2.7
CUR-ARG$^-$-HYD	7.68	5.9	0.45 (at 40 – 100 °C)	1.7

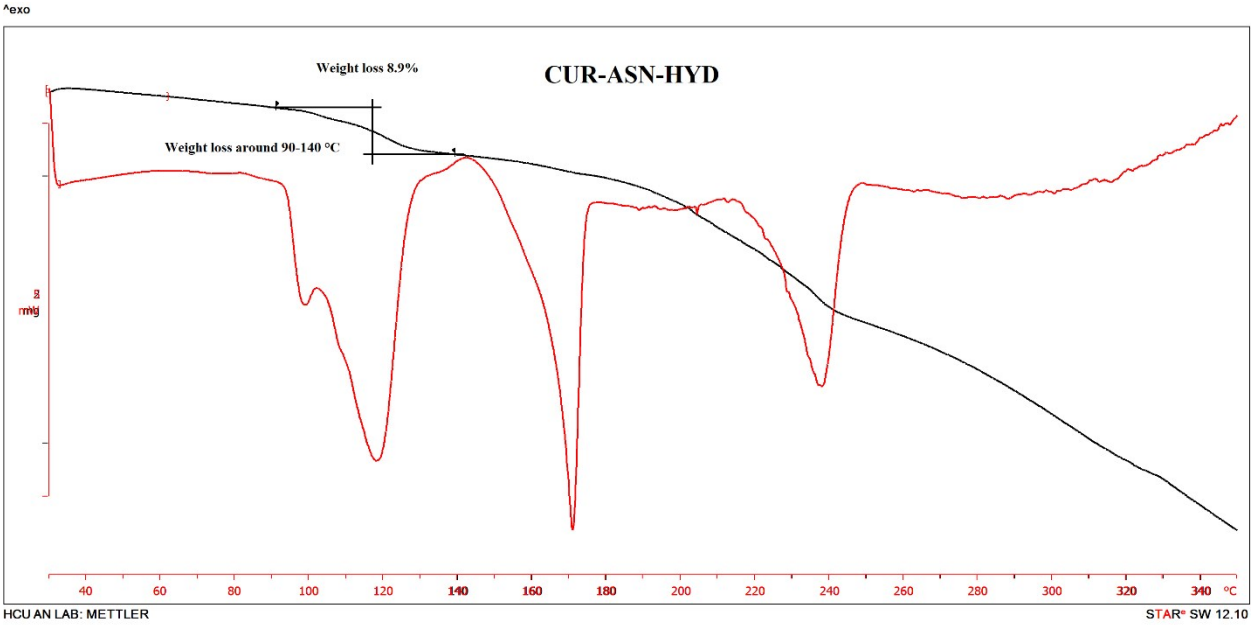

Figure S2a: DSC and TGA comparison of CUR-ASN-HYD

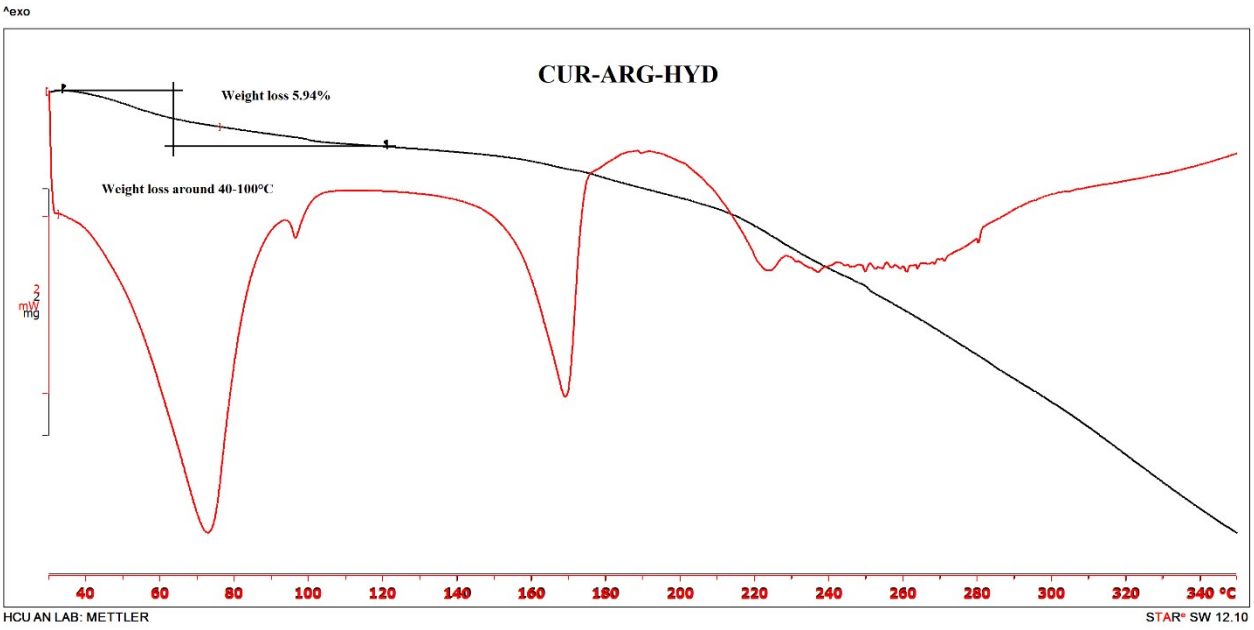

Figure S2b: DSC and TGA comparison of CUR-ARG-HYD

Table S2: Experimental Solidus Temperatures (TS) and Liquidus Temperatures (TL) of CUR−TYR Binary System as a Function of Curcumin Mole Fraction at 0.25 MPa. CUR Forms a Eutectic with TYR at a Mole Fraction of 0.25.

Mole fraction of curcumin (X_{CUR})	Solidus temp (TS) (in °C)	Liquidus temp (TL) (in °C)
0	--	159.74
0.10	103.85	140.73
0.20	103.4	--
0.25	102.7	--
0.33	104.09	--
0.40	99.82	122.38
0.50	103.78	124.19
0.67	98.33	129.6
0.75	99.65	131.39
0.80	105.46	143.75
0.90	107.95	152.46
1	--	165.37

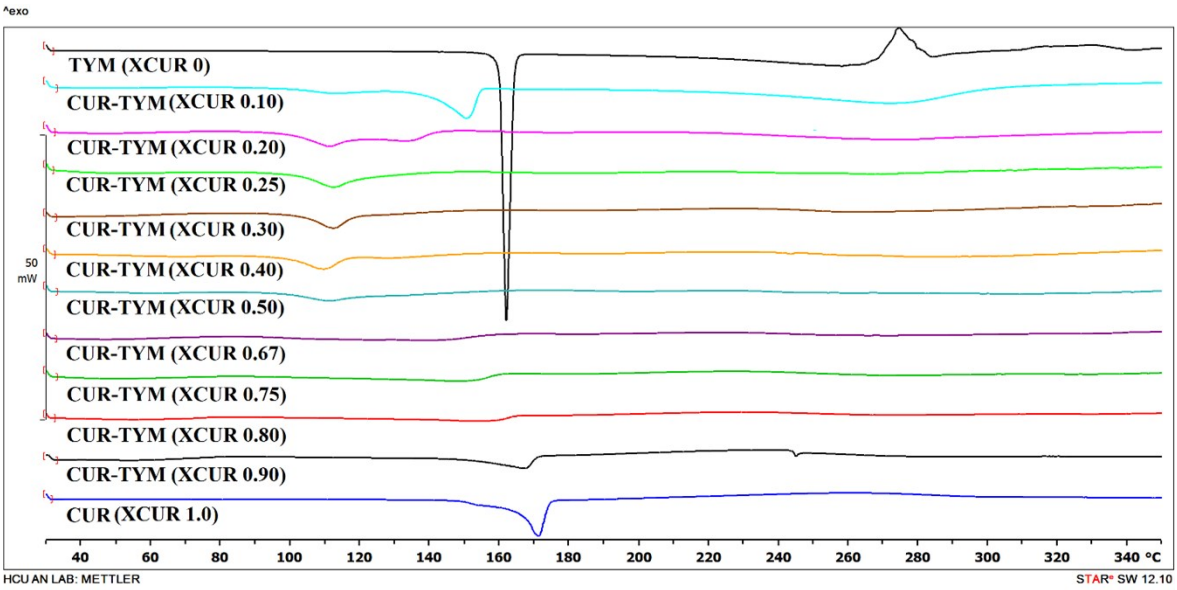

Figure S3: DSC thermogram of CUR-TYM eutectic with different mole fraction of CUR.

Chemical Shift of CUR amino acid solid forms in NMR spectra:

CUR ^{1}H NMR (DMSO-D_6): 3.83 (6H, s), 6.0 (1H, s), 6.74-6.83 (5H, m), 7.14-7.15 (4H, m), 7.32-7.56 (3H, m), 9.68 (1H, s).
TYM ^{1}H NMR (DMSO-D_6): 2.50 (2H, t), 2.6 (2H, t), 3.35 (1H, s), 6.6 (2H, d) and 6.9 (2H, d).3.3(1H, s).
CUR-TYR ^{1}H NMR (DMSO-D_6 & Methanol-D_4): 2.50 (2H, t), 2.7 (2H, t), 3.8 (6H, s), 6.0 (1H, s), 6.6 (3H, d), 6.7 (3H, d), 6.9 (2H, d), 7.1 (2H, d), 7.2 (2H, s) and 7.5 (3H, d).

TPM ^{1}H NMR (DMSO-D_6): 2.7 (2H, t), 2.8 (2H, t), 6.9 (1H, t), 7.0 (1H, t), 7.1 (1H, s), 7.3 (1H, d), 7.5 (1H, d) and 10.8 (1H, s).

CUR-TPM co-amorphous ^{1}H NMR (DMSO-D_6 & Methanol-D_4): 2.8 (2H, d), 3.0 (2H, s), 3.8 (6H, s), 6.6 (4H, s), 6.7 (2H, d), 6.9 (2H, s), 7.0 (1H, s), 7.1 (3H, s), 7.2 (2H, d), 7.3 (2H, d), 7.5 (2H, d), 10.9 (1H, s) and 11.4 (1H, s).

CUR-TPM cocrystal ^{1}H NMR (DMSO-D_6 & Methanol-D_4): 2.8 (2H, d), 3.0 (2H, s), 3.8 (6H, s), 6.6 (4H, s), 6.7 (2H, d), 6.9 (2H, s), 7.0 (1H, s), 7.1 (3H, s), 7.2 (2H, d), 7.3 (2H, d), 7.5 (2H, d), 10.9 (1H, s) and 11.4 (1H, s).

ARG ^{1}H NMR (D_2O): 1.40-1.44 (4H, m), 2.99-3.02 (2H, t), 3.07-3.08 (1H, t).

CUR-ARG ^{1}H NMR (DMSO-D_6 and D_2O): 1.56 (4H, m), 3.20 (3H, m), 3.79 (6H, m), 6.49-6.70 (4H, m), 6.98-7.08 (4H, m), 7.35-7.47 (3H, m).

CUR-ARG-HYD ^{1}H NMR (DMSO-D_6 and D_2O): 1.48-1.61 (4H, m), 3.03 (2H, s), 3.21 (1H, s), 3.71 (6H, s), 6.55-6.68 (5H, m), 7.00-7.09 (4H, m), 7.39 (3H, m).

ASN ^{1}H NMR (D_2O): 2.6 (1H, m), 2.7 (1H, m), 3.7 (1H, t).

CUR-ASN-HYD ^{1}H NMR (DMSO-D_6 & D_2O): 2.7 (2H, d), 3.6 (1H, s), 3.7 (6H, s), 6.5 (2H, d), 6.7 (3H, s), 7.0 (4H, d), 7.3 (3H, s).

GLN ^{1}H NMR (D_2O): 2.0 (2H, m), 2.3 (2H, m), 3.6 (1H, t).

CUR-GLN ^{1}H NMR (DMSO-D_6 & D_2O): 1.9 (2H, m), 2.2 (2H, m), 3.4 (1H, t), 3.7 (6H, s), 6.6 (2H, d), 6.7 (3H, s), 7.0 (4H, d), 7.4 (3H, s).

LYS ^{1}H NMR (D_2O): 1.3 (2H, m), 1.6 (2H, m), 1.7 (2H, m), 2.9 (2H, t), 3.5 (1H, t).

CUR-LYS ^{1}H NMR (DMSO-D_6 & D_2O): 1.3 (2H, s), 1.5 (2H, m), 1.6 (2H, m), 2.7 (2H, m), 3.3 (1H, t), 3.7 (6H, s), 6.6 (2H, s), 6.7 (3H, s), 7.0 (4H, d), 7.4 (3H, s).

HIS ^{1}H NMR (D2O): 2.8-3.0(2H, m), 3.7 (1H, m), 6.8 (1H, s), 7.5 (1H, s).

CUR-HIS ^{1}H NMR (DMSO-D_6 & D_2O): 2.8-3.0 (2H, m), 3.6 (1H, m), 3.7 (6H, s), 6.6 (2H, m), 6.7 (3H, d), 6.8 (2H, m), 7.1 (2H, m), 7.4 (3H, m) and 7.6 (1H, s).

CIT ^{1}H NMR (D_2O): 1.3 (2H, m), 1.6 (2H, m), 2.9 (2H, s), 3.5 (1H, s).

CUR-CIT ^{1}H NMR (DMSO-D_6 & D_2O): 1.4 (2H, m), 1.7 (2H, m), 2.9 (2H, s), 3.3 (1H, s).3.7 (6H, s), 6.6 (2H, s), 6.7 (3H, s), 7.0 (4H, d), 7.4 (3H, s).

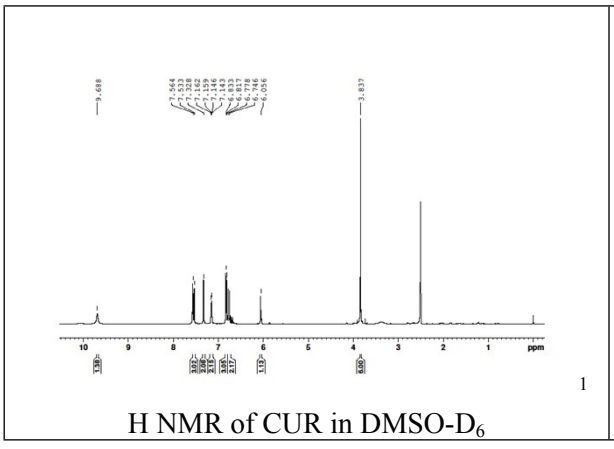

H NMR of CUR in DMSO-D_6

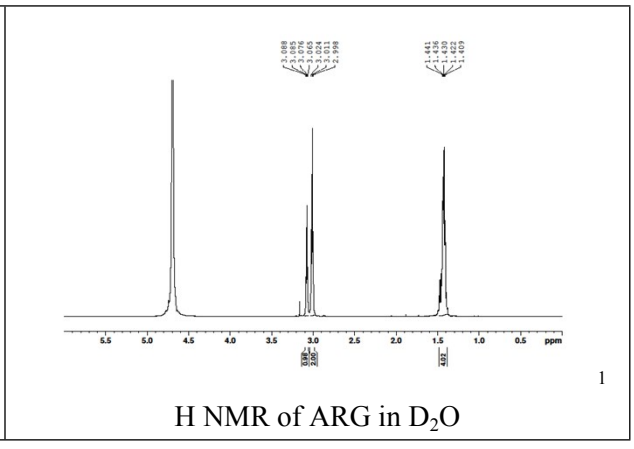

H NMR of ARG in D_2O

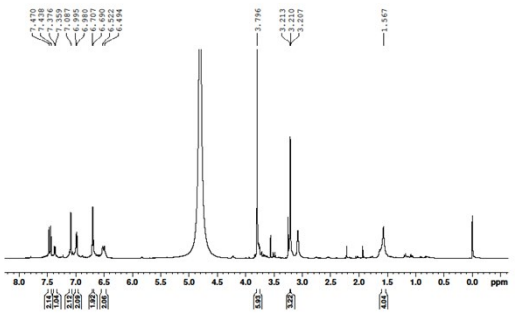

^{1}H NMR of CUR-ARG in DMSO-D_6 and D_2O

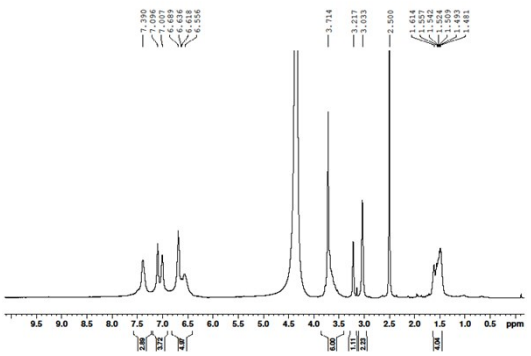

^{1}H NMR of CUR-ARG-HYD in DMSO-D_6 and D_2O

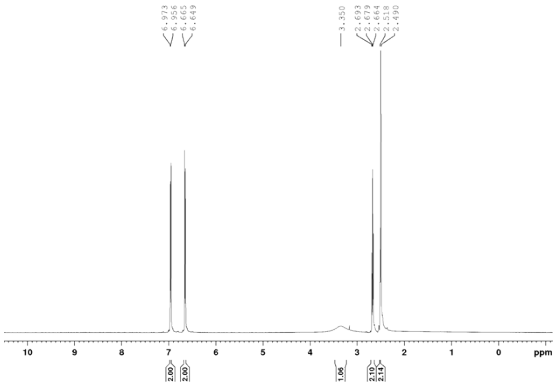

^{1}H NMR of TYM in D_2O

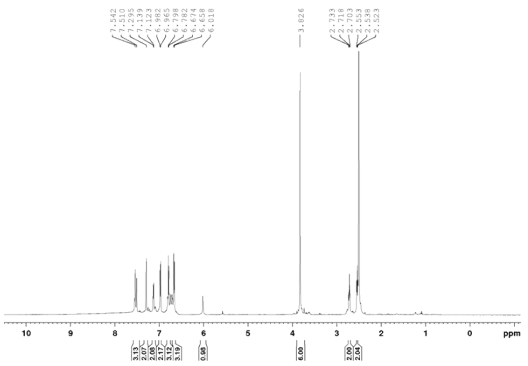

^{1}H NMR of CUR-TYM in DMSO-D_6 and Methanol-D_4.

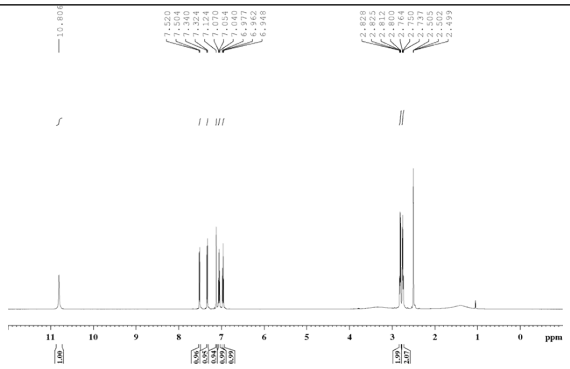

^{1}H NMR of TPM in DMSO-D_6.

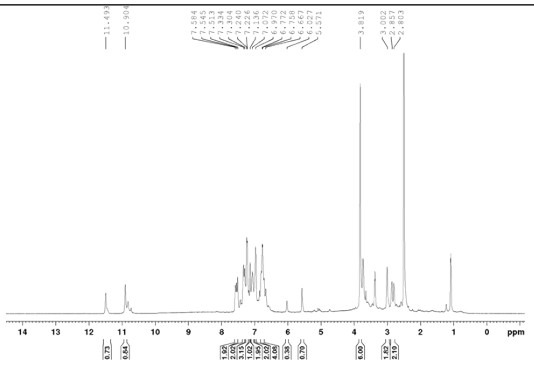

^{1}H NMR of CUR-TPM in DMSO-D_6 and Methanol-D_4.

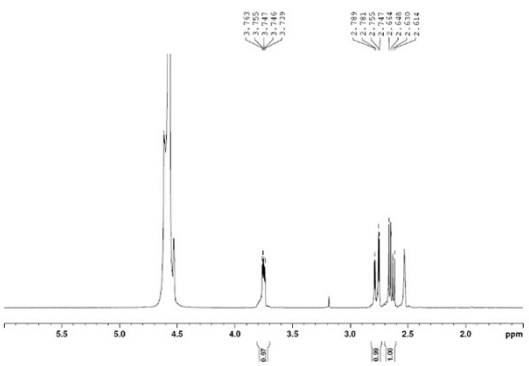

^{1}H NMR of ASN in D_2O & DMSO-D_6.

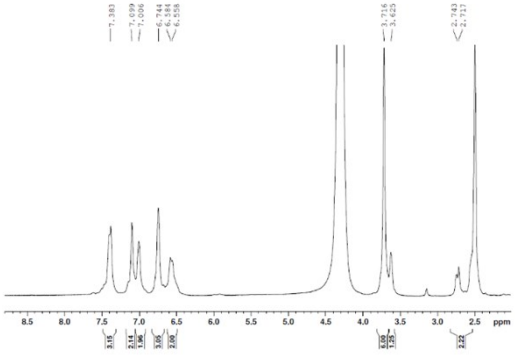

^{1}H NMR of CUR-ASN-HYD in D_2O & DMSO-D_6.

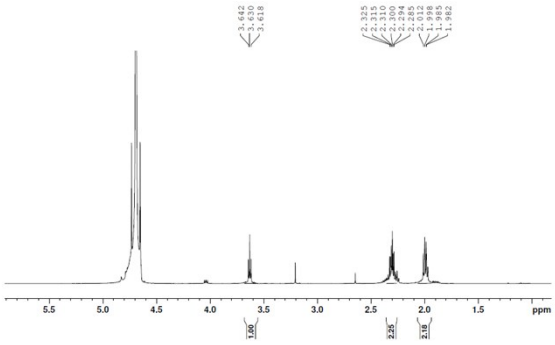

^{1}H NMR of GLN in D_2O.

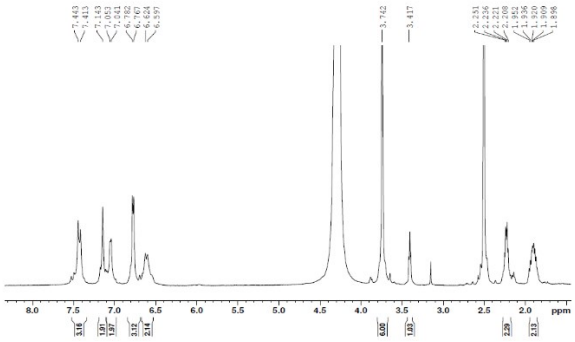

^{1}H NMR of CUR-GLN in D_2O & DMSO-D_6.

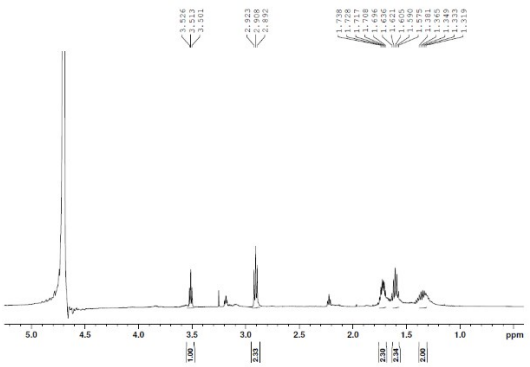

^{1}H NMR of LYS in D_2O.

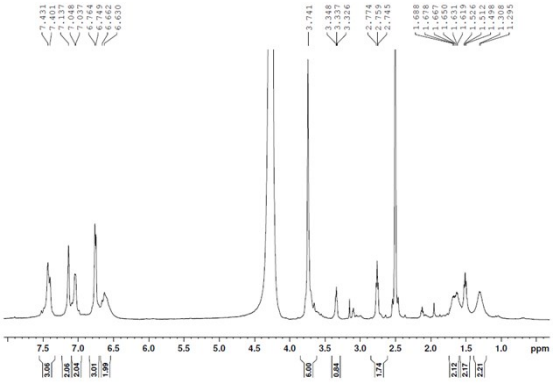

^{1}H NMR of CUR-LYS in D_2O & DMSO-D_6.

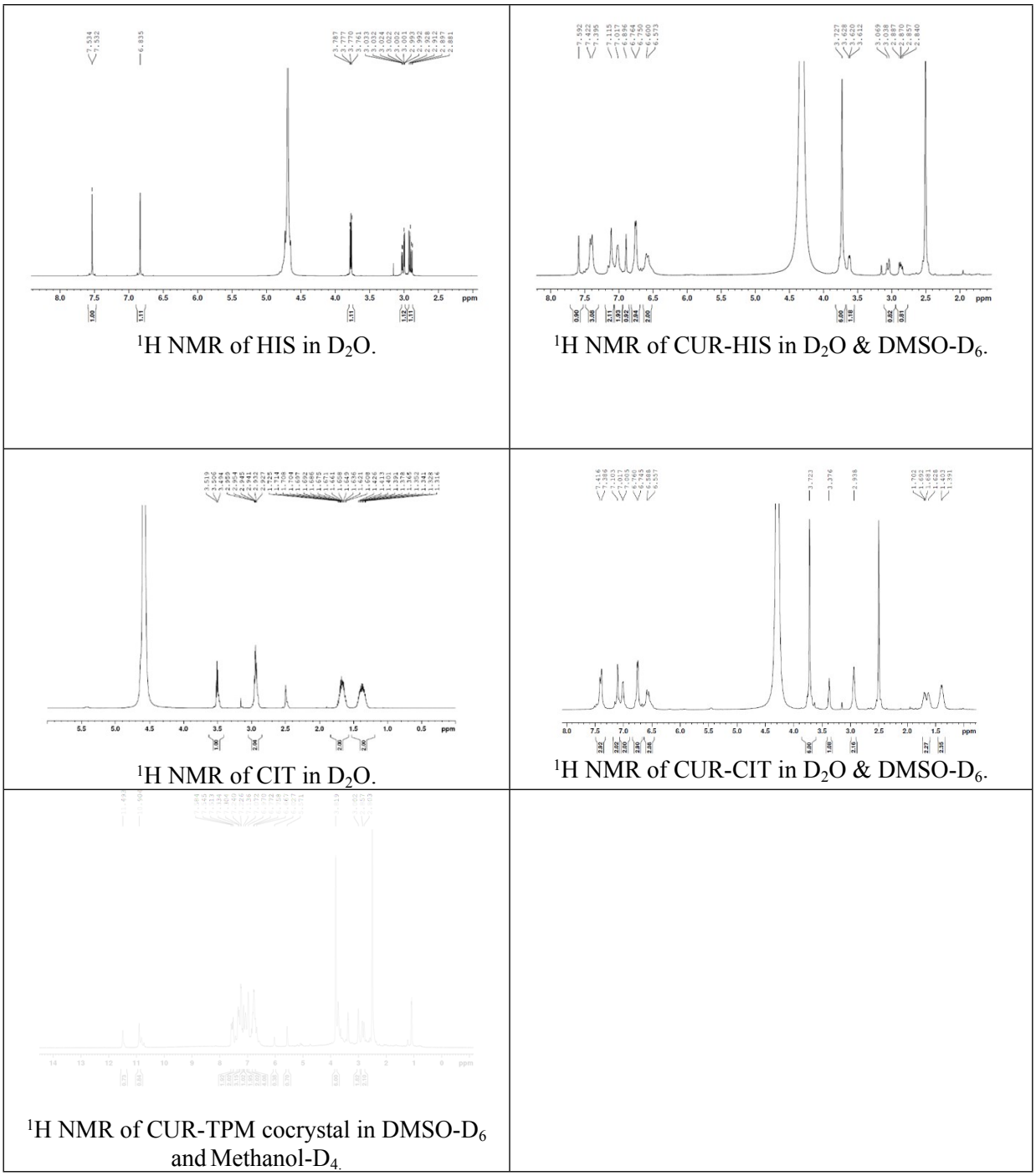

^{1}H NMR of HIS in D_2O.

^{1}H NMR of CUR-HIS in D_2O & DMSO-D_6.

^{1}H NMR of CIT in D_2O.

^{1}H NMR of CUR-CIT in D_2O & DMSO-D_6.

^{1}H NMR of CUR-TPM cocrystal in DMSO-D_6 and Methanol-D_4.

Figure S4: ^{1}H NMR of CUR and its coformers along with binary mixtures.

FT-IR Spectroscopy:

There was not much change in the shifts of stretching frequencies in curcumin and its binary mixtures to confirm them as cocrystals as its formation involves a structural change. However, the small change in the stretching frequencies of curcumin functional groups in new binary solids indicates that the newly formed binary solid phases are not so stable in the lattice due to lack of strong interactions or misfit/mismatch in

the crystal lattice results in the formation of eutectic (CUR-TYM) or co-amorphous (CUR-TPM) systems. TYM has N−H_{str} 3335.4 and 3282.8cm^{-1} and phenolic C−O $_{str}$ at 1265.1 cm^{-1} which shifts to 3335.7 and 3281.8 cm^{-1} and 1265.6 cm^{-1} respectively in CUR-TYM. The shift in the stretching frequencies corresponds to enolic and phenolic hydroxyl groups 3511.4 cm^{-1}(red shift), aromatic C=C skeletal vibrations 1595.2 and 1509.7 (blue shift), C−O stretching of enolic and phenolic hydroxyl groups 1429.4 cm^{-1}(red shift) and 1281.2 cm^{-1}(blue shift) indicating new solid phase. TPM having N−H_{str} 3344.3, 3281.1 and 3135.4 cm^{-1}, which shifts to 3405.2 cm^{-1} (red shift) and in CUR moiety enolic and phenolic hydroxyl groups 3508.4 cm^{-1}(blue shift), aromatic C=C skeletal vibrations 1571.4 and 1511.8 (blue shift), C−O stretching of phenolic hydroxyl groups 1281.2 cm^{-1}(blue shift) in case of co-amorphous solid, whereas in cocrystal the stretching frequencies corresponding to hydroxyl and amine functionalities diminished. The carbonyl stretching frequency in cocrystal is blue shifted to 1619.7 cm^{-1}.

ARG exhibits functional group stretching frequency for N−H_{str} 3358.6 and 2863.5 cm^{-1} and carboxylate COO^- $_{str}$ 1560.0 and 1421.3 cm^{-1} respectively. The red shift in stretching frequency of enolic and phenolic hydroxyl groups 3511.4 cm^{-1}, carbonyl group 1627.6 cm^{-1}, aromatic C=C skeletal vibrations 1603.3, 1509.0 cm^{-1} and C−O stretching of enolic and phenolic hydroxyl groups 1429.0 cm^{-1} and 1281.2 cm^{-1} corresponds to CUR and N−H_{str} 3361.2-2863.8 cm^{-1} and carboxylate COO^- $_{str}$ 1559.8 and 1429.3 corresponds to ARG in CUR-ARG binary mixture.

ASN has amine and carboxyl stretching bands at 3376.0 cm^{-1} and 3127.0 cm^{-1} which are shifted to 3381.7 cm^{-1}, 3108.1 cm^{-1} in CUR-ASN-HYD physical mixture. The phenolic hydroxyl groups and carbonyl groups in CUR are blue shifted to 3505.5 cm^{-1} and red shifted to1629.3 cm^{-1} respectively. The enolic and phenolic C-O shifts are also observed in CUR-ASN. GLN has amine stretching frequency at 3410.4, 3317.1, 3214.5 and carbonyl/carboxylate stretching at 1630.2 which are shifted to 3405.4, 3210.4 and 1629.3. Similarly, the phenolic hydroxyl groups and carbonyl groups in CUR are red shifted to 3512.8cm^{-1} and red shifted to1629.3 cm^{-1} respectively. The enolic and phenolic C-O shifts are also observed in CUR-GLN. LYS having amine stretching frequency at 3359.0 cm^{-1}, 3066.9 $cm^{-1}$and carbonyl/carboxylate stretching at 1639.2 cm^{-1} which are shifted to 3355.4, 2943.3 and 1602.3 cm^{-1} respectively. The phenolic hydroxyl groups and carbonyl groups in CUR are blue shifted to 3505.8cm^{-1} and red shifted to 1628.2 cm^{-1} respectively. The enolic and phenolic C-O shifts are also observed in CUR-LYS. HIS is having amine stretching frequency at 3143.4 cm^{-1} and carbonyl/carboxylate stretching at 1624.7 cm^{-1}, 1588.6 cm^{-1} which are shifted to 3015.6 cm^{-1} and 1586.3 cm^{-1} respectively. The phenolic hydroxyl groups and carbonyl groups in CUR are red shifted to 3513.3 cm^{-1} and red shifted to 1629.1 cm^{-1} respectively. The enolic and phenolic C-O shifts are also observed in CUR-HIS. CIT is having amine stretching frequency at 3358.8 cm^{-1}, 3189.1 cm^{-1} and carbonyl/carboxylate stretching at 1675.5 cm^{-1}, 1639.2 cm^{-1} which are shifted to 3341.3 cm^{-1}, 3045.8 cm^{-1} and respectively. The phenolic hydroxyl groups and carbonyl groups in CUR are blue shifted to 3509.8cm^{-1} and blue shifted to 1627.4 cm^{-1} respectively. The enolic and phenolic C-O shifts are also observed in CUR-CIT.

From the shifts in stretching frequencies of three different multicomponent binary solid forms CUR-ARG and CUR-TYM showing red shift in O−H stretching frequencies corresponds to the formation of new eutectic systems. The CUR-TPM showing blue shift for O−H_{str} corresponds to co-amorphous formation.

Table S3: FT-IR frequency of CUR and binary solid forms.

	O−H	**C=O**	**Aromatic C=C**	**Enol C−O**	**Phenol C−O**	**N−H**	**COO^-**
CUR	3510.9	1627.5	1602.6 1509.8	1429.0	1281.2	--	--
ARG	--	--	--	--	--	3358.6, 3299.4, 2944.8, 2863.5	1560.0, 1421.3
CUR-ARG	3511.4	1627.6 1678.9 1721.7	1603.3 1509.0	1429.3	1281.7	3361.2, 3297.4, 2940.3, 2863.8	1559.8, 1429.3
CUR-ARG-HYD	3508.4	1627.6 1678.9	1603.1 1510.6	1429.1	1281.8	3301.9	1565.7
TYM	--	--	1594.8	--	1265.1	3335.4, 3282.8	--
CUR-TYM	3511.4	1627.5	1595.2 1509.7	1429.4	1265.6	3335.7, 3281.8	--
TPM	--	--	1591.7	--	--	3344.3,3281.1 3135.4	--
CUR-TPM-Coamorphous	3508.4	1627.9	1571.4 1511.8	1429.0	1279.9	3405.2	--
CUR-TPM-Cocrystal	--	1619.7	1572.5 1492.6 1459.2	1422.2	1255.5	3262.8, 2912.9	--
ASN	--	--	--	--	--	3376.0 3127.0, 2928.2	1683.4 1640.2
CUR-ASN-HYD	3505.5	1629.3	1577.4 1508.5	1429.8	1277.2	3381.7, 3108.1	1602.7 1570.8
GLN	--	--	1577.2	--	--	3410.4, 3317.1 3214.5	1689.3 1630.2 1580.4
CUR-GLN	3512.8	1629.3	1603.1 1583.3 1512.1	1428.9	1282.2	3405.4, 3210.4	1686.8 1629.3 1583.3
LYS	--	--	--	--	--	3359.0, 3066.9 2948.2, 2860.8	1639.2 1581.5
CUR-LYS	3505.8	1628.2	1602.3 1583.3	1429.7	1282.1	3355.4, 2943.3	1602.3 1583.3
HIS	--	--	--	--	--	3143.4	1624.7 1588.6
CUR-HIS	3513.3	1629.1	1602.9 1586.3	1429.3	1281.3	3015.6	1586.3
CIT	--	--	--	--	--	3358.8, 3189.1 3046.4, 2963.9	1675.5 1639.2 1548.6
CUR-CIT	3509.8	1627.4	1603.0 1580.4	1429.4	1281.3	3341.3, 3045.8	1676.0 1549.2

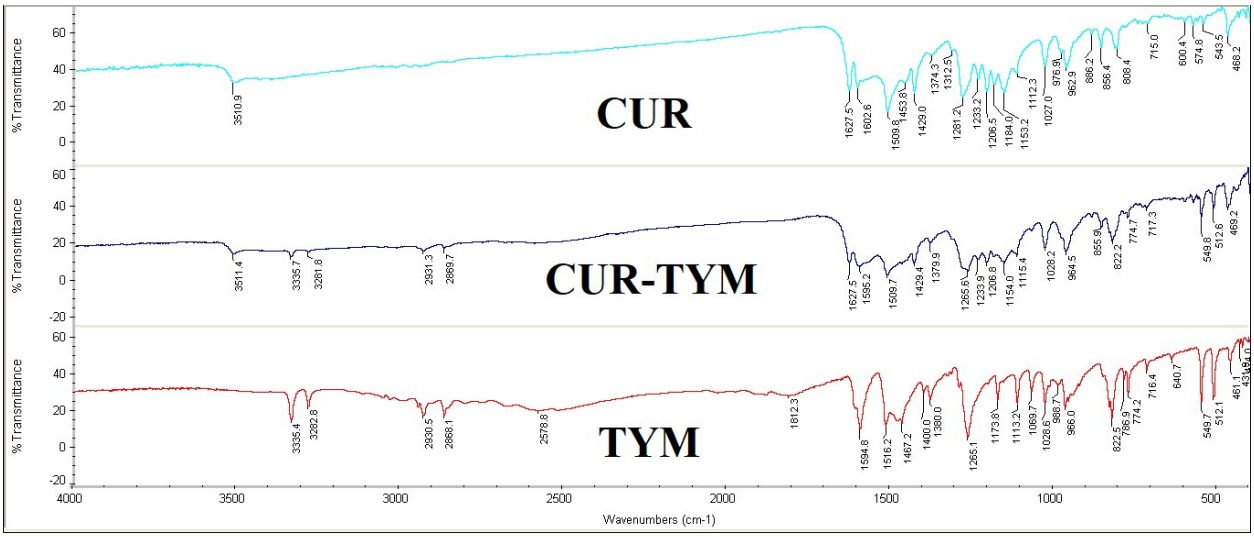

Figure S5a: IR spectra of CUR-TYM eutectic system in comparison with CUR and TYM

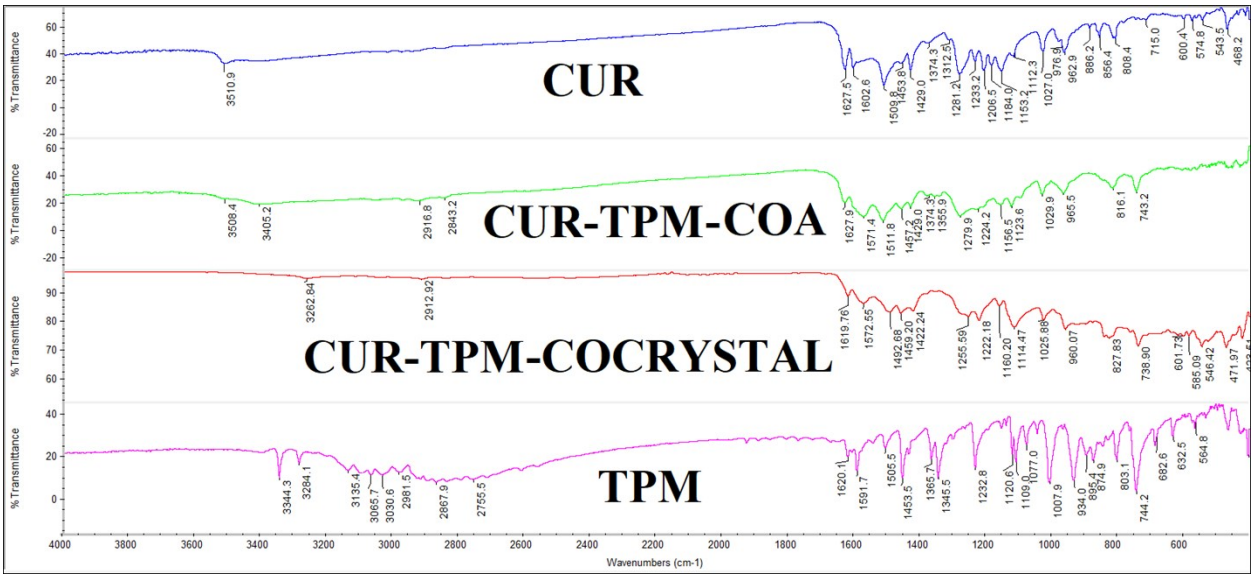

Figure S5b: IR spectra of CUR-TPM co-amorphous and CUR-TPM cocrystal in comparison with CUR and TPM

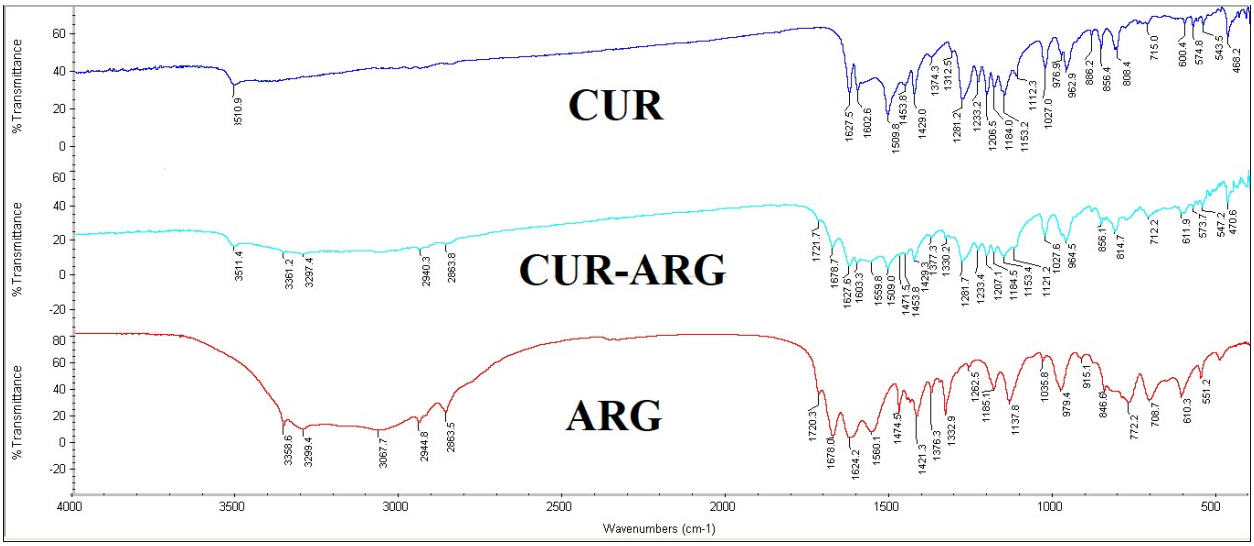

Figure S5c: IR spectra of CUR-ARG physical mixture in comparison with CUR and ARG

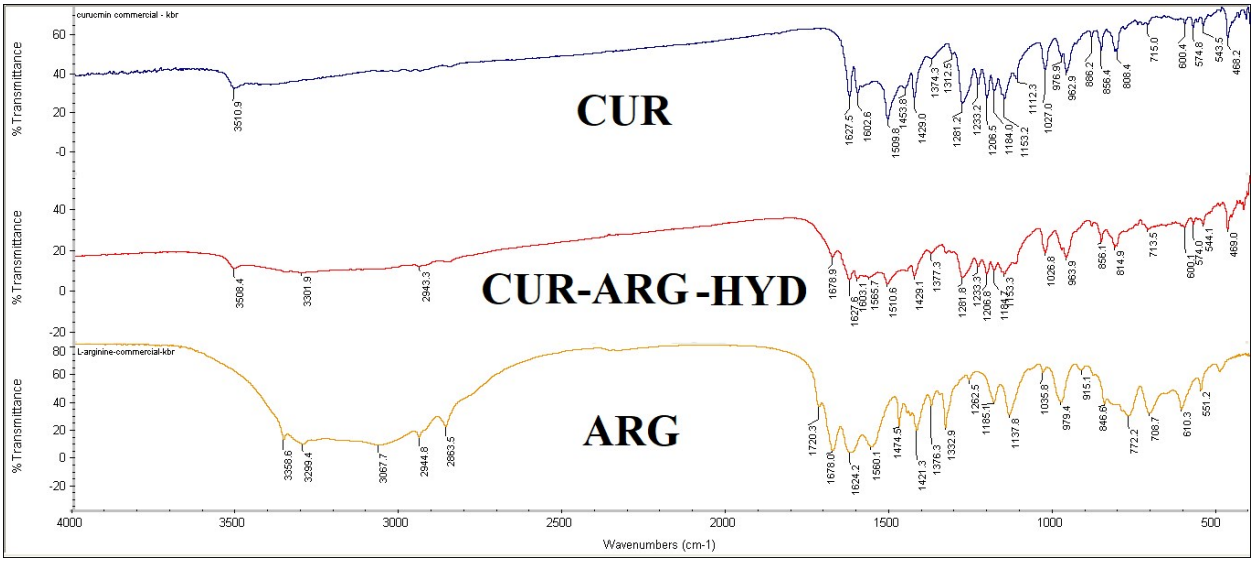

Figure S5d: IR spectra of CUR-ARG-HYD physical mixture in comparison with CUR and ARG.

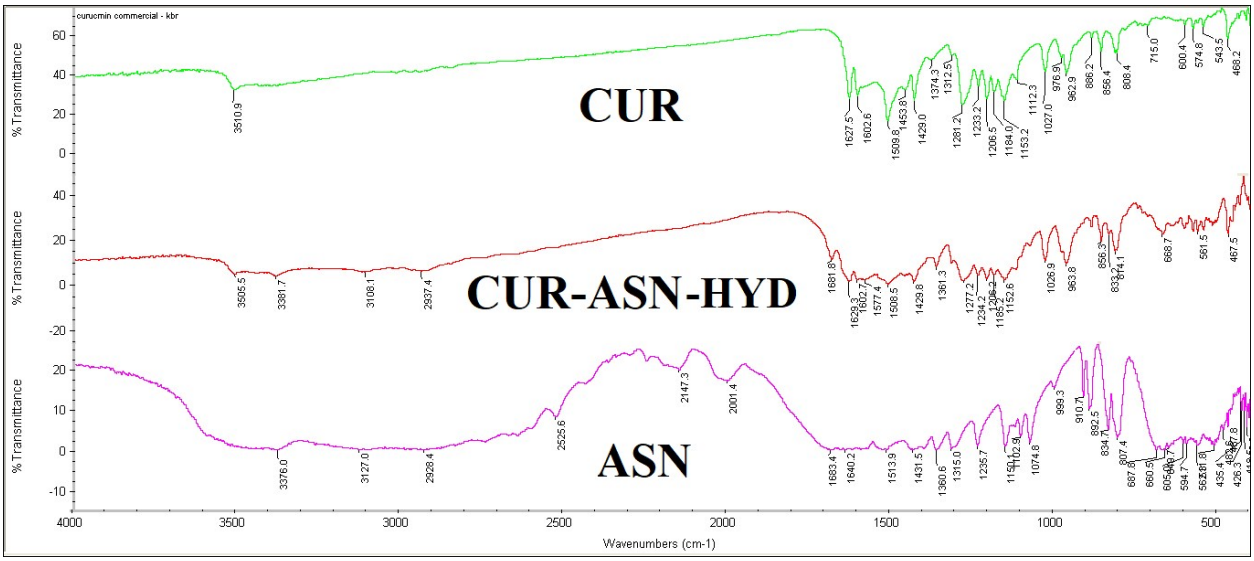

Figure S5e: IR spectra of CUR-ASN-HYD physical mixture in comparison with CUR and ASN

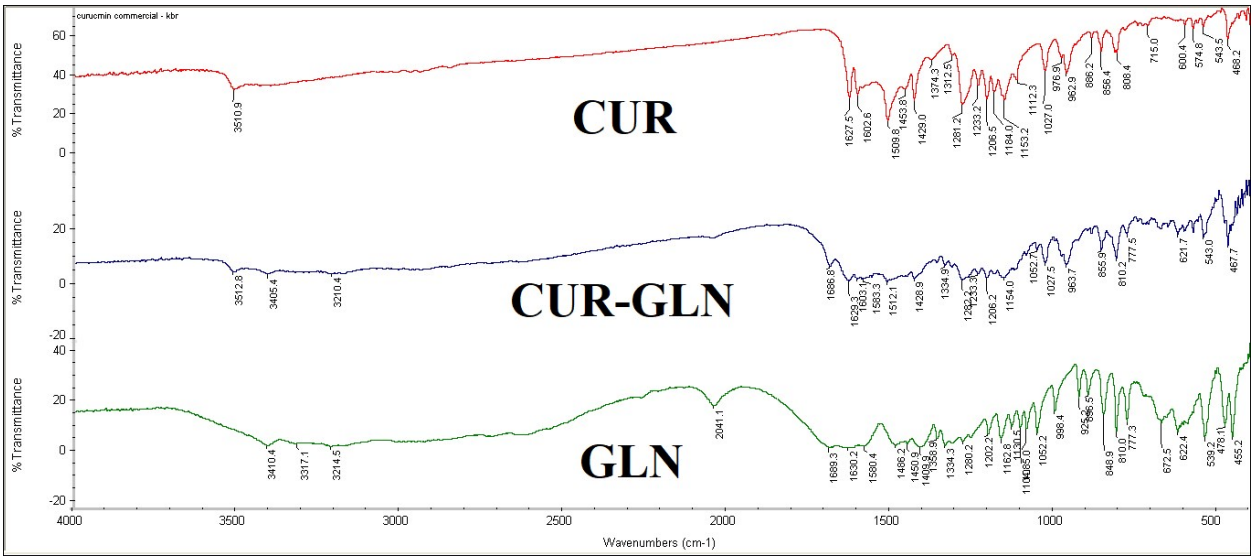

Figure S5f: IR spectra of CUR-GLN physical mixture in comparison with CUR and GLN

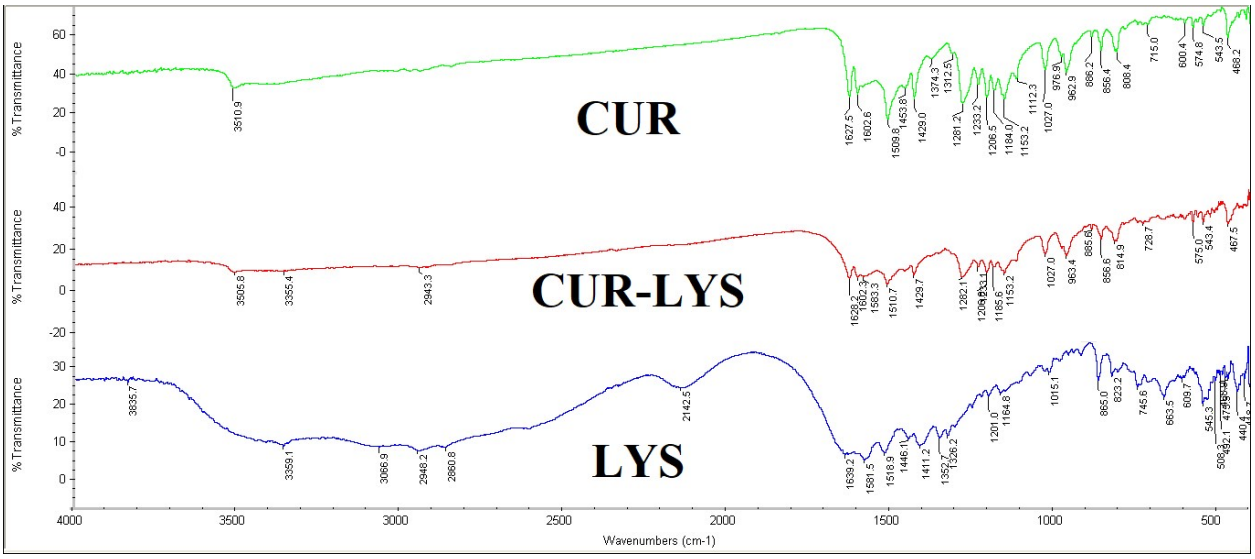

Figure S5g: IR spectra of CUR-LYS physical mixture in comparison with CUR and LYS.

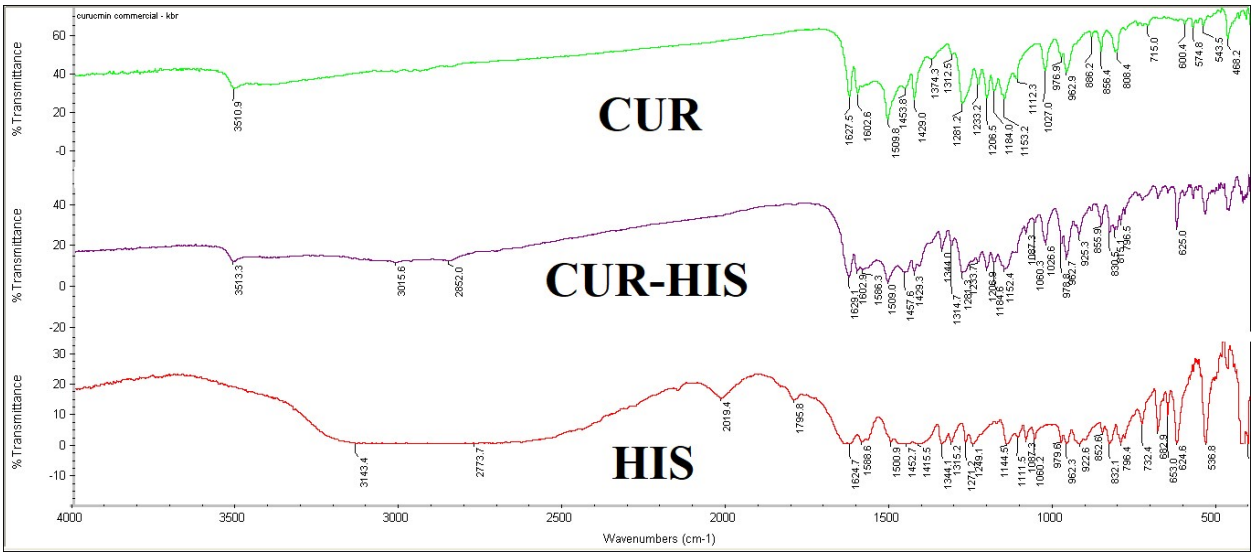

Figure S5h: IR spectra of CUR-HIS physical mixture in comparison with CUR and HIS.

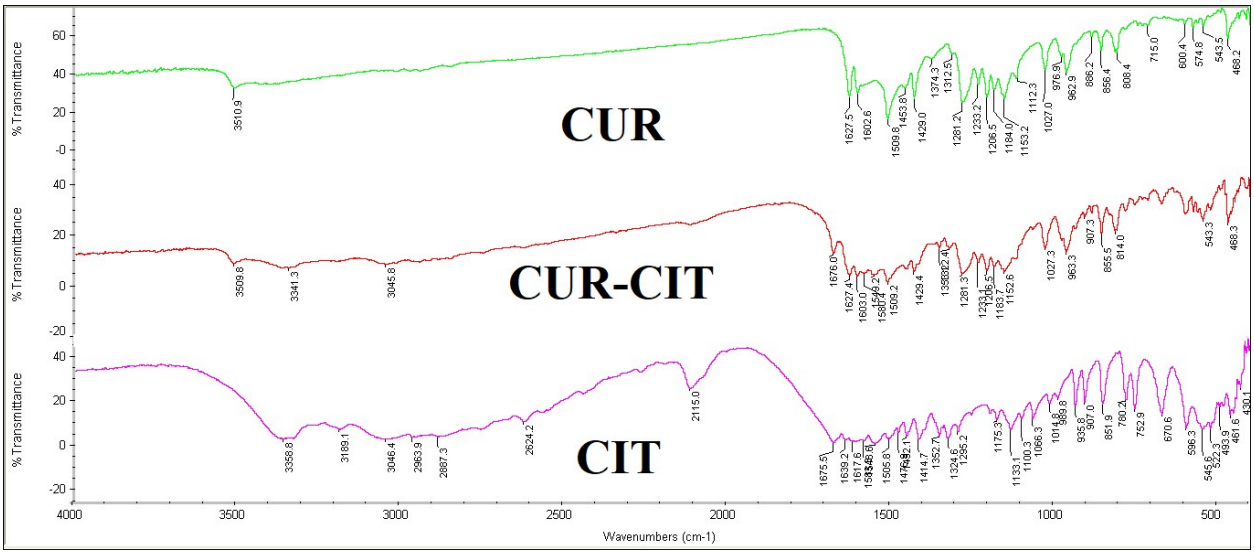

Figure S5i: IR spectra of CUR-CIT physical mixture in comparison with CUR and CIT.

Figure S5: FT-IR spectral overlay of CUR solid forms (sample prepared as KBr pellet).

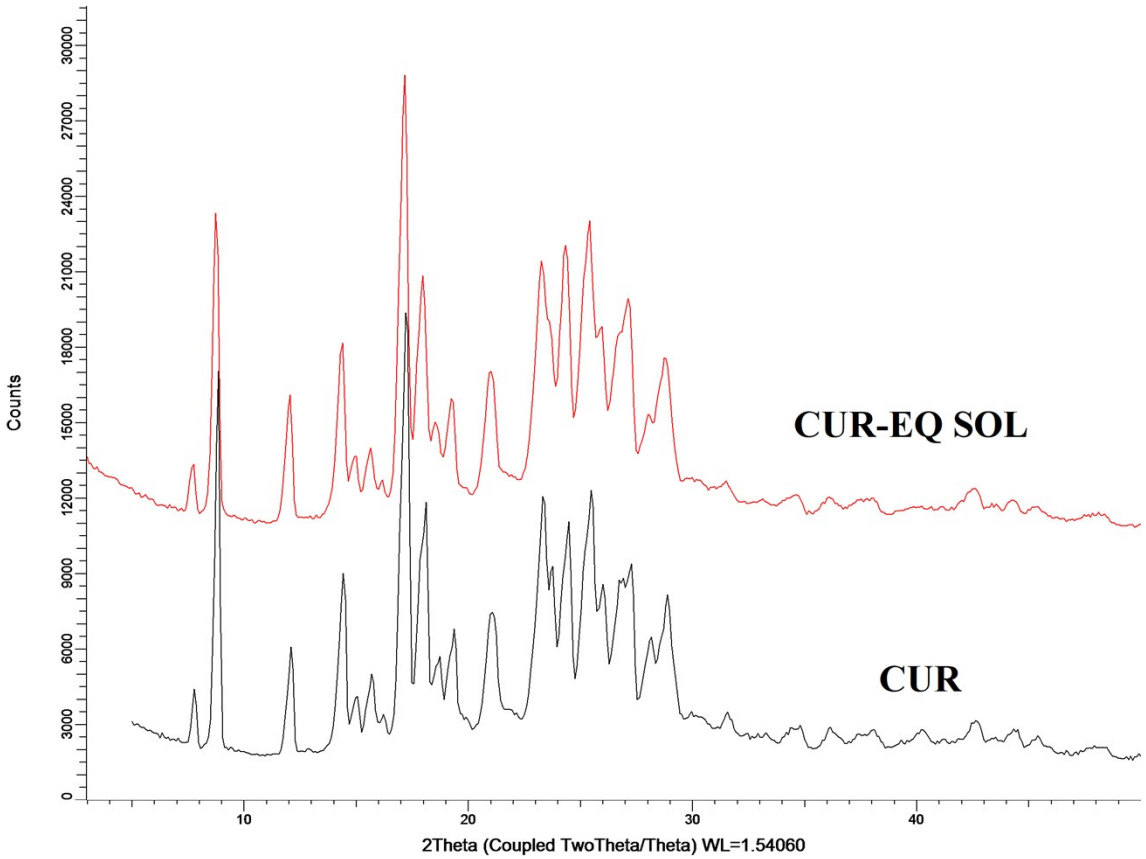

Figure S6a: PXRD overlay of CUR before (black) and after equilibrium solubility experiment(red) in 40% ethanol-water medium.

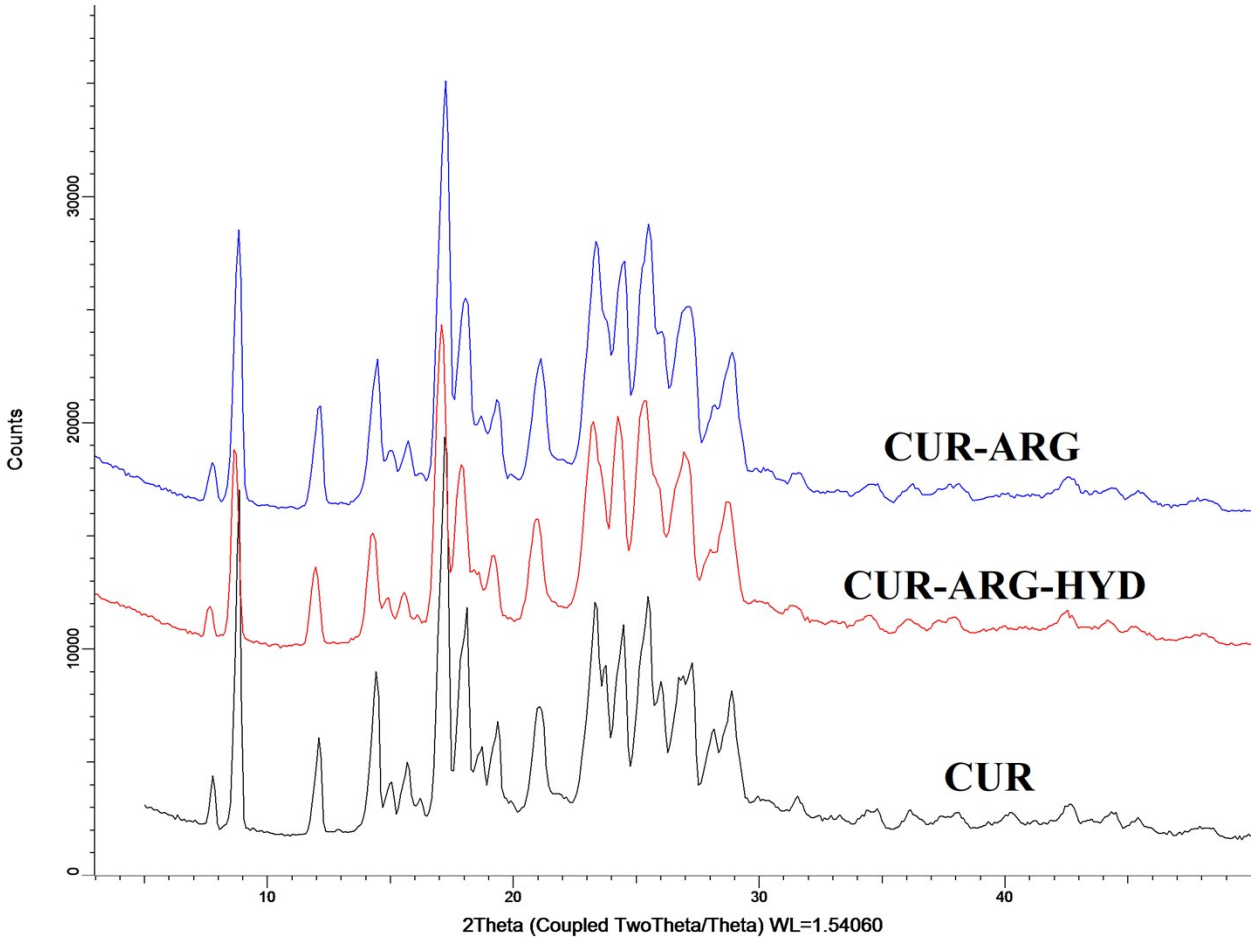

Figure S6b: PXRD overlay of CUR-ARG (blue) and CUR-ARG-HYD (red) after the equilibrium solubility experiment with pure CUR (black) in 40% ethanol-water medium.

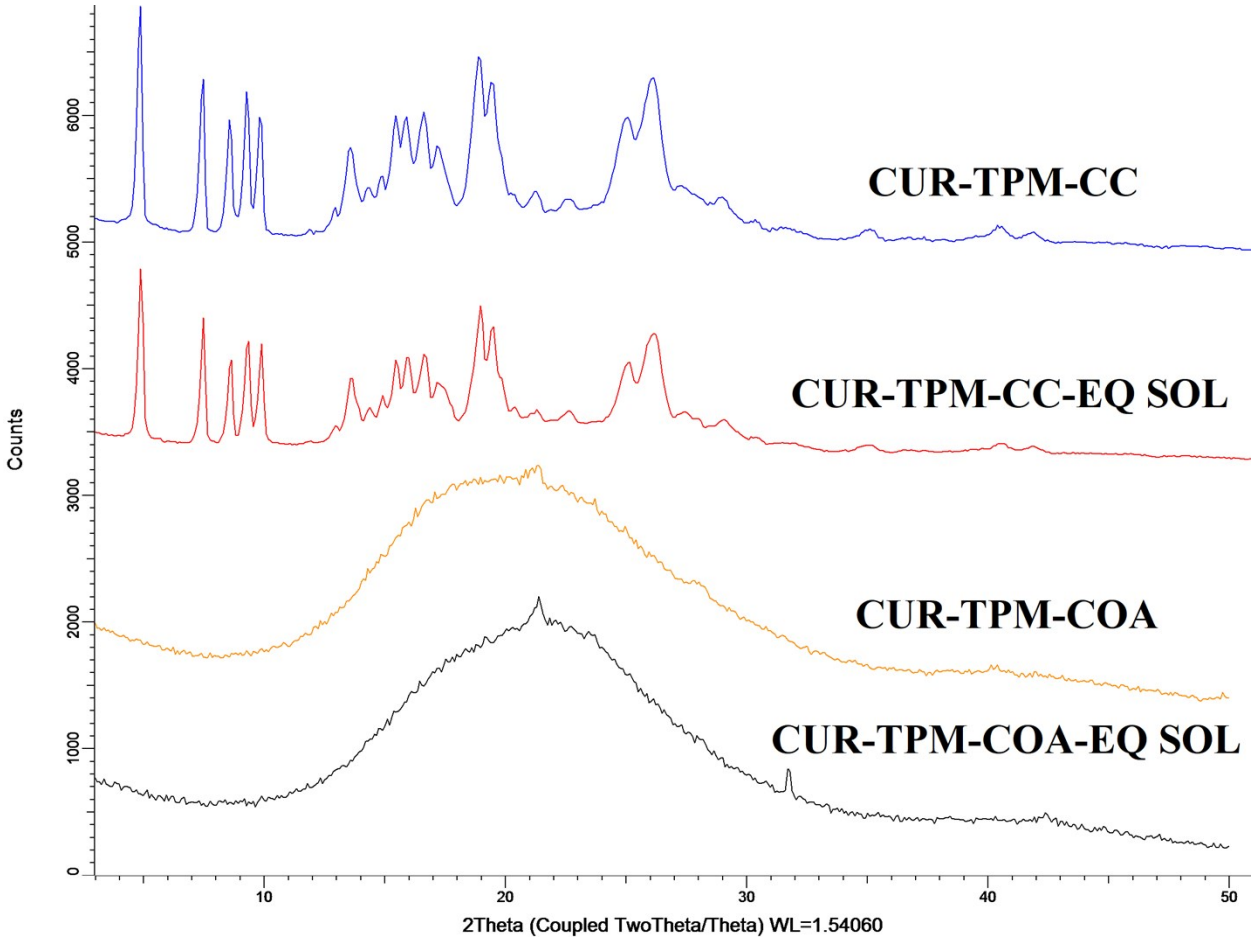

Figure S6c: PXRD overlay of CUR-TPM cocrystal starting material (blue) and CUR-TPM coamorphous starting material (yellow) after the equilibrium solubility experiment of CUR-TPM cocrystal (red) and CUR-TPM coamorphous (black) in 40% ethanol-water medium indicating their phase stability.

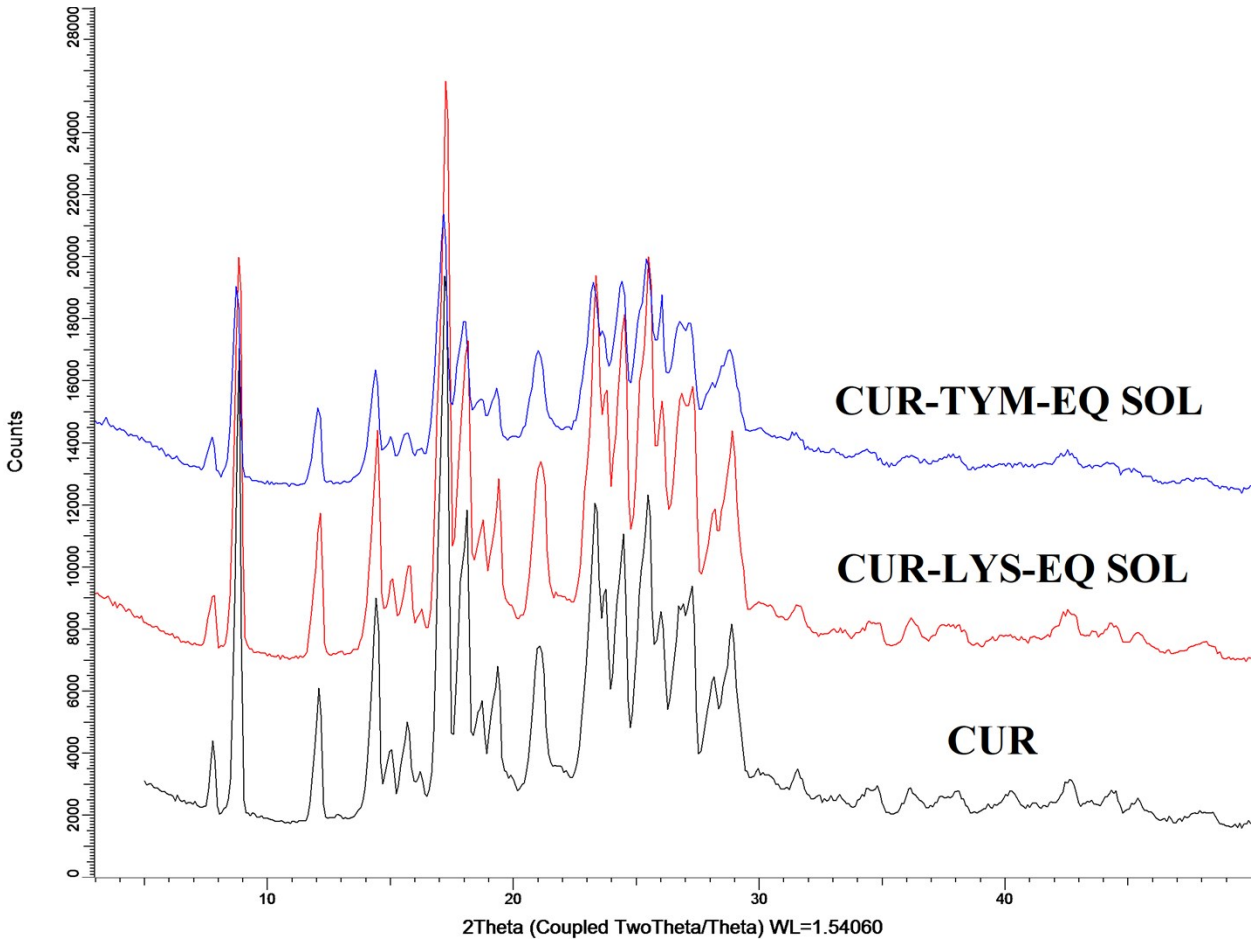

Figure S6d: PXRD overlay of CUR-TYM (blue) and CUR-LYS (red) after the equilibrium solubility experiment with pure CUR (black) in 40% ethanol-water medium.

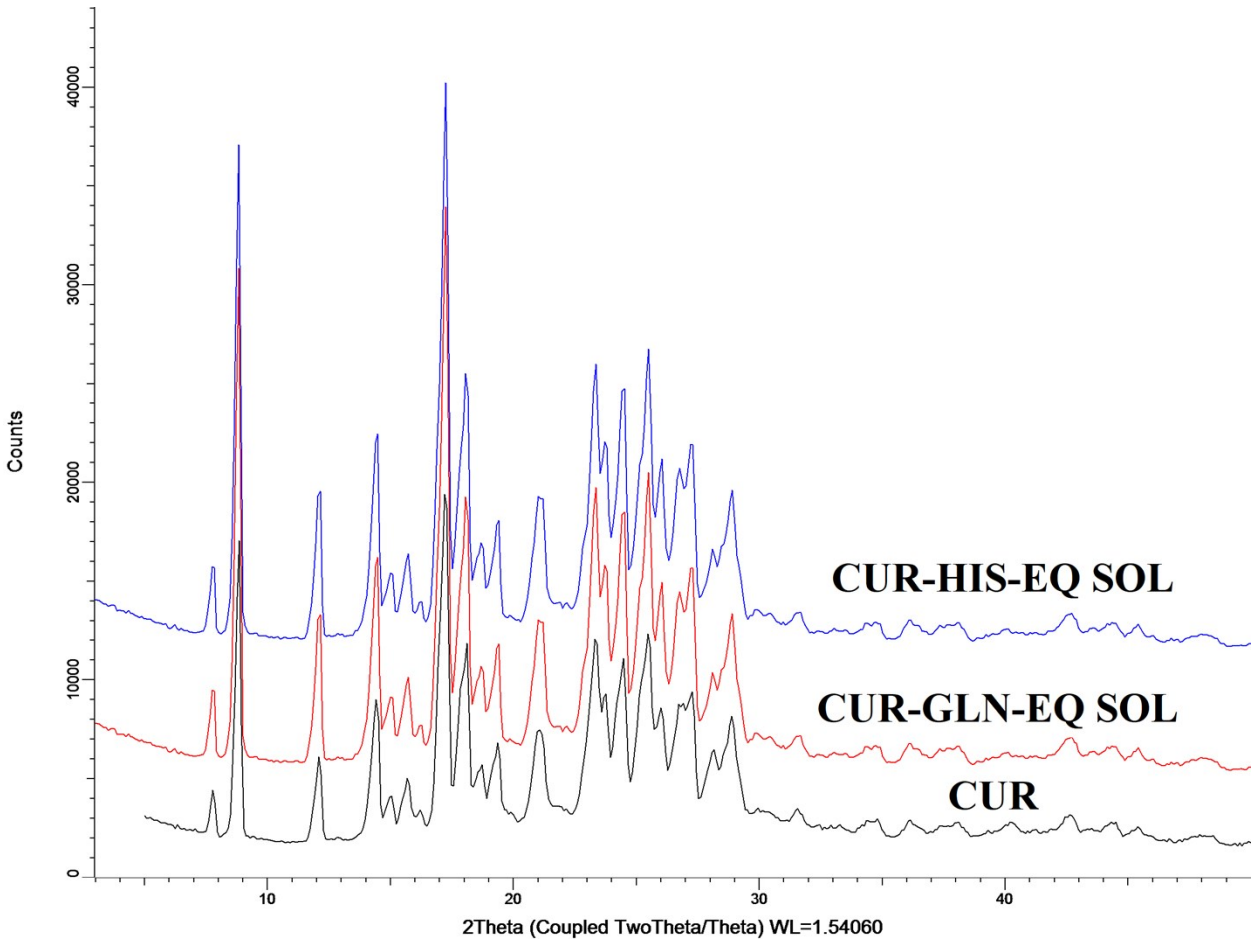

Figure S6e: PXRD overlay of CUR-HIS (blue) and CUR-GLN (red) after the equilibrium solubility experiment with pure CUR (black) in 40% ethanol-water medium.

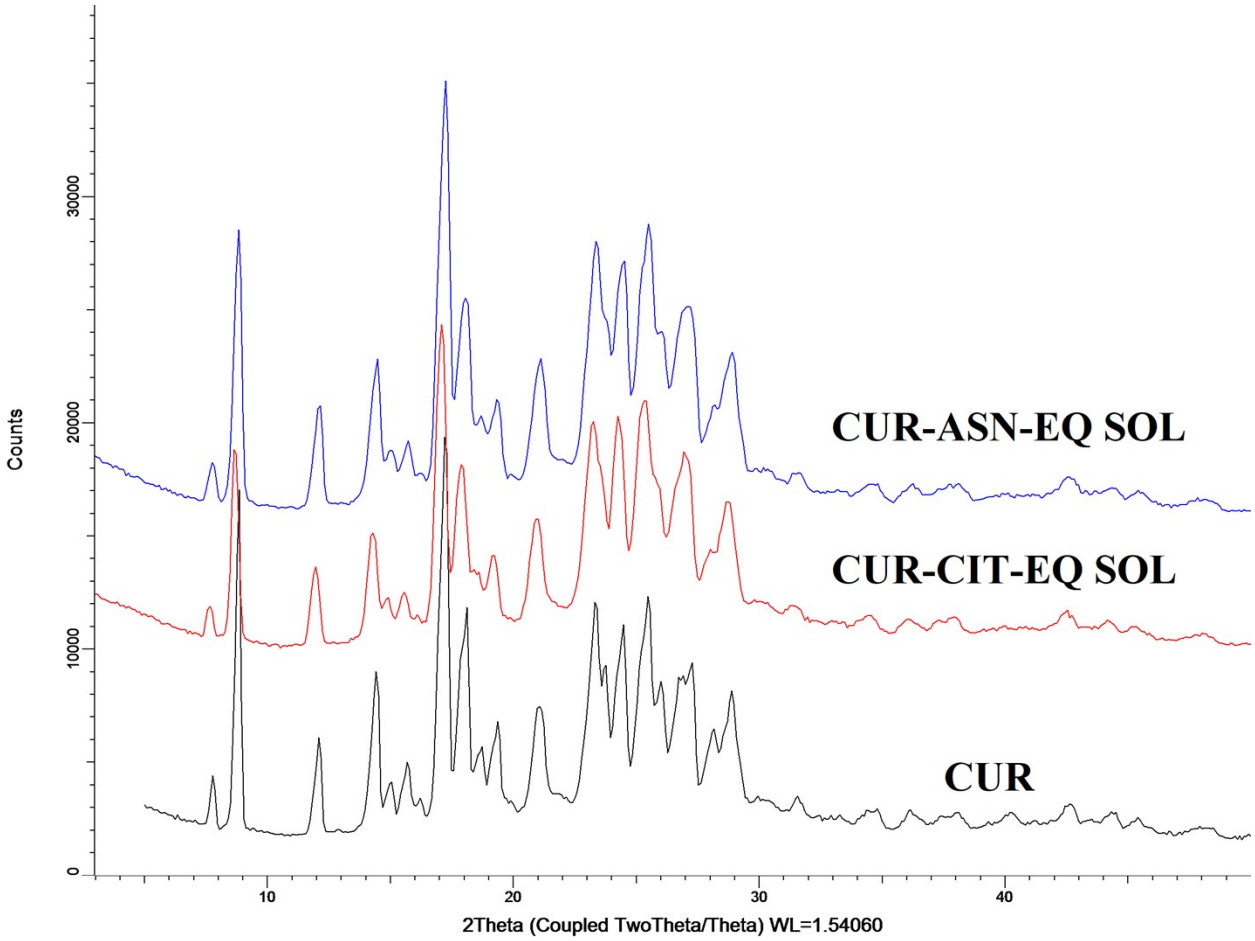

Figure S6f: PXRD overlay of CUR-ASN (blue) and CUR-CIT (red) after the equilibrium solubility experiment with pure CUR (black) in 40% ethanol-water medium.

Figure S6: PXRD overlay of CUR and its solid forms after equilibrium solubility experiment (black) in 40% ethanol-water medium.

Table S4: pH changes during the dissolution experiment of CUR and its solid forms.

Time (min)	pH of the dissolution medium (40% ethanol-water)										
	CUR	CUR-ARG	CUR-ARG-HYD	CUR-TPM-COA	CUR-TPM-CC	CUR-TYM	CUR-LYS	CUR-ASN	CUR-GLN	CUR-HIS	CUR-CIT
0	7.26	7.26	7.26	7.26	7.26	7.26	7.26	7.26	7.26	7.26	7.26
15	6.85	4.42	400	4.72	5.38	5.63	4.86	4.99	5.32	5.60	5.06
30	6.85	6.30	6.06	5.88	5.53	5.42	6.51	6.23	6.32	6.42	6.23
60	6.76	6.00	6.26	5.45	5.00	5.26	6.25	5.98	6.06	6.42	6.09
90	6.83	5.78	6.48	5.35	5.044	5.10	5.98	5.85	5.86	5.80	5.92
120	6.70	5.48	6.04	5.05	4.95	4.63	5.56	5.68	5.58	5.01	5.87
150	6.89	5.30	5.87	4.80	4.60	4.79	5.32	5.40	5.90	4.71	5.72
180	6.53	4.93	5.82	4.59	4.49	4.52	5.20	5.36	5.75	4.40	5.68
240	6.69	4.85	5.56	4.90	4.93	4.88	4.99	5.28	5.68	4.42	5.62
300	6.90	5.12	5.57	4.62	4.72	4.22	4.81	5.40	5.36	4.36	5.48
360	6.56	4.95	519	4.35	4.33	4.69	4.69	5.32	5.22	4.49	5.62
420	6.42	4.66	5.29	4.33	4.22	4.30	4.52	5.33	5.65	4.48	5.52
480	6.35	4.50	5.12	4.39	4.35	4.20	4.52	5.29	5.25	4.10	5.46